Free Radical Biology & Medicine 49 (2010) 214–226

Contents lists available at ScienceDirect

Free Radical Biology & Medicine

journal homepage: www.elsevier.com/locate/freeradbiomed

Original Contribution

Flavokawain B, a novel chalcone from *Alpinia pricei* Hayata with potent apoptotic activity: Involvement of ROS and GADD153 upstream of mitochondria-dependent apoptosis in HCT116 cells

Yu-Feng Kuo [a], Ying-Zhen Su [a], Yen-Hsueh Tseng [b], Sheng-Yang Wang [b], Hsi-Ming Wang [a], Pin Ju Chueh [a,*]

[a] *Graduate Institute of Biomedical Sciences, National Chung Hsing University, Taichung 40227, Taiwan, Republic of China*
[b] *Department of Forestry, National Chung Hsing University, Taichung 40227, Taiwan, Republic of China*

ARTICLE INFO

Article history:
Received 30 June 2009
Revised 18 March 2010
Accepted 8 April 2010
Available online 14 April 2010

Keywords:
Apoptosis
Alpinia pricei Hayata
Anticancer
Flavonoid
Flavokawain B
GADD153
ROS
Free radicals

ABSTRACT

Flavonoids synthesized from chalcone precursors in plants have been shown to possess cytotoxic activities with therapeutic potential. We have isolated the novel chalcone flavokawain B from *Alpinia pricei* Hayata, a plant native to Taiwan that is used in food and traditional Chinese medicine. Here, we report for the first time that flavokawain B significantly inhibits the growth of colon cancer cells and provide novel insight into the molecular mechanisms that underlie its apoptotic activity. Flavokawain B exerts its apoptotic action through ROS generation and GADD153 up-regulation, which lead to mitochondria-dependent apoptosis characterized by release of cytochrome *c* and translocation of Bak. The up-regulation of GADD153 in flavokawain B-treated HCT116 cells is associated with mitochondrial dysfunction and altered expression of Bcl-2 family members. Moreover, pretreatment with the ROS scavenger *N*-acetylcysteine abolishes flavokawain B-induced ROS generation, GADD153 up-regulation, and apoptosis. Similarly, RNAi-mediated gene silencing reduced flavokawain B-enhanced expression of GADD153 and apoptotic Bim, leading to diminished apoptosis. Interestingly, flavokawain B provokes G2/M accumulation as well as autophagy, in addition to apoptosis, suggesting that multiple pathways are activated in flavokawain B-mediated anticancer activity. Taken together, our data provide evidence for a molecular mechanism to explain the apoptotic activity of *Alpinia* plants, showing that flavokawain B acts through ROS generation and GADD153 up-regulation to regulate the expression of Bcl-2 family members, thereby inducing mitochondrial dysfunction and apoptosis in HCT116 cells.

Natural products have been utilized as novel compounds for the treatment of many diseases, including cancer, because of their ability to inhibit cancer cell growth and induce apoptosis [1–4]. Among the compounds that have been suggested to possess antiproliferative activities with therapeutic potential are the flavonoids, which are synthesized from chalcone precursors in plants and composed of two benzene rings joined by a linear three-carbon chain [5–8]. The antiproliferative potential of chalcone in the extract of kava kava, a plant grown in the Pacific Islands, has been inferred from the correlation between high kava consumption and a lower incidence of cancer [9,10]. The chalcone flavokawain A, in particular, has been shown to induce cytotoxicity in bladder cancer cells by promoting Bax activation and subsequent mitochondria-dependent apoptosis [11].

Much attention has focused on apoptosis as an important cell-death pathway, especially for its prominent role in cancer inhibition. Apoptosis is a complex process that occurs in response to a variety of stress stimuli, and the extrinsic pathway of apoptosis is dependent on ligand binding to a death receptor followed by the formation of a death-inducing signaling complex, which subsequently activates caspase-8 and effector caspases [12]. An alternative intrinsic pathway has also been identified. This mitochondria-dependent mechanism is characterized by translocation of Bax/Bak to mitochondria and release of cytochrome *c* from mitochondria into the cytoplasm. These mitochondrial alterations subsequently activate a caspase cascade that induces an ordered series of events, culminating in degradation of the cell [13–17].

Recent findings have shed light on the importance of other organelles involved in integrating apoptotic signaling to initiate caspase activation and apoptosis; in particular, stress in the endoplasmic reticulum (ER) reflected by the unfolded-protein response and abnormal calcium homeostasis has been implied [18–20]. One of the many proteins induced as part of the adaptive ER stress response is

Abbreviations: BAPTA, 1,2-bis(2-aminophenoxy)ethane-*N*,*N*,*N*′,*N*′-tetraacetic acid; $DiOC_6(3)$, dihexyloxocarbocyanine iodide (3); DPI, diphenyleneiodonium chloride; GADD153, growth arrest and DNA damage-inducible gene153; H_2DCFDA, 2′,7′-dichlorodihydrofluorescein diacetate; FB, flavokawain B; FITC, fluorescein isothiocyanate; MTT, 3-(4,5-dimethylthiazol-2-yl)-2,5-diphenyltetrazolium bromide; NAC, *N*-acetylcysteine; p38 MAPK, p38 mitogen-activated protein kinase; PARP, poly(ADP-ribose) polymerase; PEG–CAT, polyethylene glycol–catalase; PI, propidium iodide; ROS, reactive oxygen species.

* Corresponding author. Fax: +886 4 22853469.
E-mail address: pjchueh@dragon.nchu.edu.tw (P.J. Chueh).

0891-5849/$ – see front matter © 2010 Elsevier Inc. All rights reserved.
doi:10.1016/j.freeradbiomed.2010.04.005

GADD153/CHOP (growth arrest and DNA damage-inducible gene 153). This member of the CCAAT/enhancer-binding protein family of transcription factors has an essential role in regulating apoptosis [21–23] although, to date, few studies have described the relationship between GADD153 elevation and induction of apoptosis in cancer cells treated with flavonoids [24–27]. These converging signaling pathways reveal a significant role for GADD153 in regulating the apoptotic response to antiproliferative flavonoids. GADD153 functions as a transcription factor that regulates the expression of a panel of genes, including the Bcl-2 family genes Bcl-2 and Bim, which, in turn, elicit mitochondrial cell death [28,29]. Although the apoptotic consequence of flavonoid-induced elevations in GADD153 in cancer cells is evident, the detailed signaling events and underlying mechanisms are not entirely certain.

The aim of this study was to gain a better understanding of the molecular mechanism underlying the previously unknown apoptotic activity of the novel chalcone flavokawain B, isolated from *Alpinia pricei* Hayata, a perennial rhizomatous herb native to Taiwan. The leaves of *A. pricei* Hayata are frequently used for making traditional rice dumplings in Taiwan and the aromatic rhizomes are used for the treatment of common cold and abdominal discomfort. Despite it being widely consumed in many Asian countries, little is known about the bioactivity of *A. pricei*. In this study, we investigated the apoptotic activity of one chalcone flavonoid isolated from *A. pricei* and our results suggest that flavokawain B induces intracellular reactive oxygen species (ROS) generation, p38 MAPK phosphorylation, and GADD153 up-regulation, leading to mitochondria-dependent apoptosis in human colon cancer cells.

Materials and methods

Materials

Rhizomes of *A. pricei* were collected in Ping-Tung County, Taiwan, in March 2007 and identified by Dr. Yen-Hsueh Tseng (National Chung Hsing University). A voucher specimen was deposited in the herbarium of the same university. Air-dried rhizomes of *A. pricei* (2.0 kg) were extracted exhaustively with 70% ethanol (EtOH) at ambient temperature. Total crude EtOH extract was concentrated under vacuum to yield a residue (166 g) and then partitioned

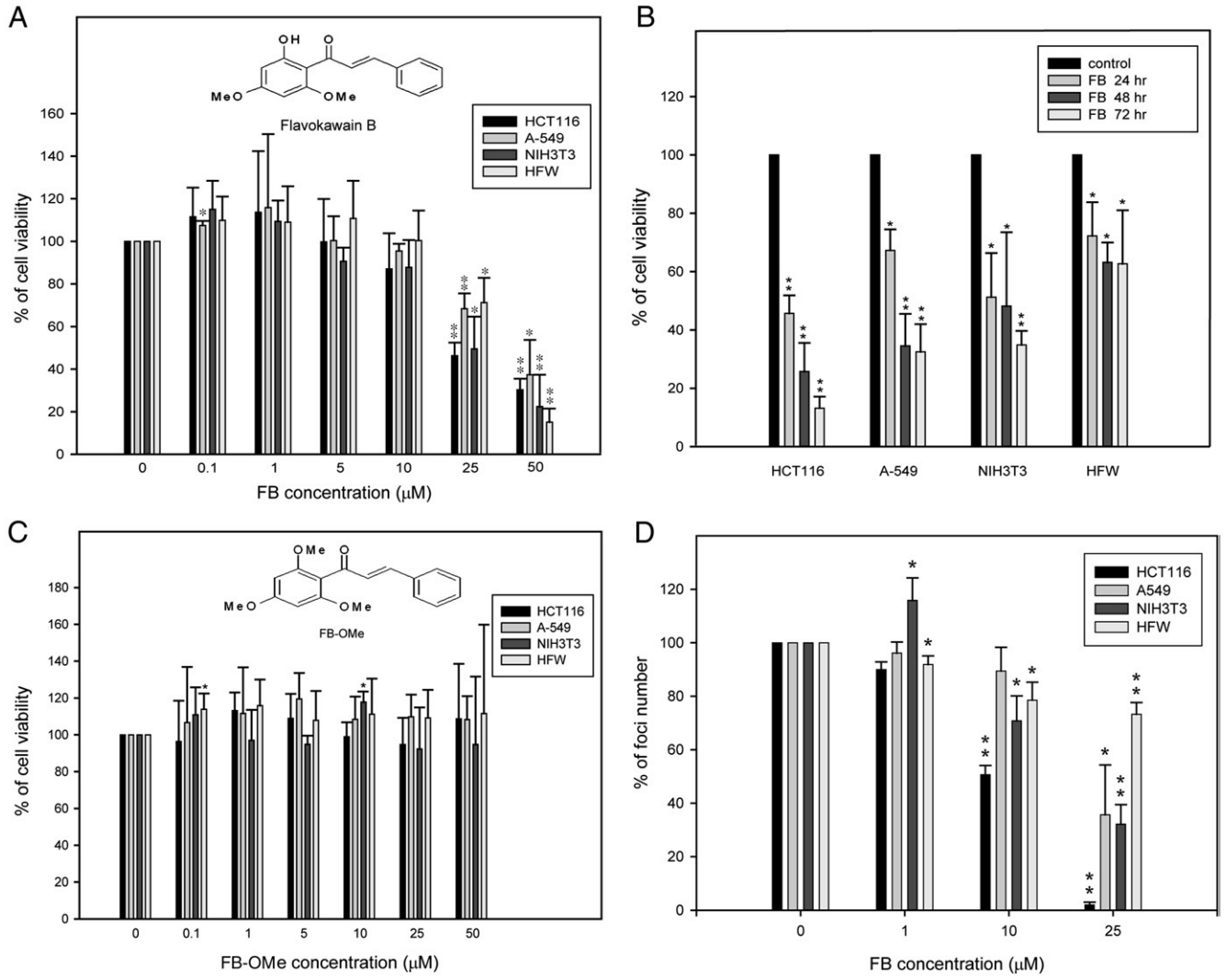

Fig. 1. Flavokawain B inhibited cell viability and proliferation in a concentration- and time-dependent manner. (A) Cells were exposed to various concentrations of flavokawain B for 24 h and cell viability was measured using MTT assays. (B) Cells were exposed to 25 μM flavokawain B for 24–72 h and cell viability was measured using MTT assays. (C) Cells were exposed to various concentrations of FB-OMe for 24 h and cell viability was measured using MTT assays. Values (means ± SE) are from at least three independent experiments. There was a significant decrease in cell viability in cells treated with flavokawain B compared with controls (*$p<0.05$, **$p<0.01$). (D) Cells were seeded at 200 cells per dish, treated with/without flavokawain, and allowed to form colonies. Colony numbers were counted and recorded. Values (means ± SE) are from three independent experiments. There was a significant decrease in colony numbers in cells treated with flavokawain B compared with controls (*$p<0.05$, **$p<0.01$).

between ethyl acetate (EtOAc)–H_2O to give an EtOAc-soluble fraction (17.7 g) and an H_2O-soluble fraction. The EtOAc-soluble fraction was further separated by chromatography over silica gel (60–80 mesh) and eluted with an *n*-hexane/EtOAc gradient (*n*-hex:EtOAc, 95:5, 90:10, 85:15, 80:20, 70:30, 60:40, 50:50, 40:60, 0:100, each 1 L) to produce 23 fractions. Those fractions were further separated by high-performance liquid chromatography using a Luna silica column (250 × 10 mm; Phenomenex, Torrance, CA, USA) and eluted with an *n*-hex/dichloromethane/EtOAc solvent system to obtain flavokawain B [30]. The structures of these compounds were elucidated and confirmed by spectroscopic analyses. UV spectra were recorded on a Jasco V-550 and IR spectra on a Bio-Rad FTS-40 spectrometer. Electron-impact mass spectrometry and high-resolution electron-impact mass spectrometry data were collected with a Finnigan MAT-958 mass spectrometer, and NMR spectra were recorded with Bruker Avance 500 and 300-MHz FT-NMR spectrometers, at 500 (^{1}H) and 75 MHz (^{13}C).

Fetal bovine serum (FBS) and penicillin/streptomycin were obtained from Gibco/BRL Life Technologies (Grand Island, NY, USA). The anti-poly(ADP) ribose polymerase (PARP), anti-Bim, anti-Bid, anti-Bcl-2, anti-pp38, and anti-rabbit IgG antibodies were purchased from Cell Signaling Technology (Beverly, MA, USA). The anti-cytochrome *c* and anti-GADD153 antibodies were purchased from Santa Cruz Biotechnology (Santa Cruz, CA, USA). The anti-β-actin and anti-Bak antibodies were from Millipore Corp. (Temecula, CA, USA). The anti-tubulin antibody was from Abcam (Cambridge, MA, USA). The FITC-conjugated anti-mouse secondary antibody, MitoTracker, and 2′,7′-dichlorodihydrofluorescein diacetate (H_2DCFDA) were from Molecular Probes (Eugene, OR, USA). The dihexyloxocarbocyanine iodide (DiOC6(3)) was purchased from Calbiochem (San Diego, CA, USA). The anti-mouse IgG antibody and all the other chemicals were purchased from Sigma Chemical Co. (St. Louis, MO, USA), unless otherwise specified.

Cell culture and transfection

Wild-type and p53$^{-/-}$ HCT116 (human colon cancer) cells were grown in McCoy's 5A medium with 10% fetal bovine serum. A-549 (human non-small-cell lung cancer), NIH3T3 (mouse fibroblast), and HFW (human fibroblast, originally derived from newborn human foreskin [31,32]) cells were cultured in DMEM containing 10% FBS. Cells were maintained at 37 °C in a humidified atmosphere of 5% CO_2 in air, and medium was replaced every 2–3 days. The HCT116 lines were generously given by Dr. Chia-Che Chang (National Chung Hsing University, Taiwan). HFW and A-549 lines were a gift from Dr. Show-Mei Chuang (National Chung Hsing University, Taiwan). The NIH3T3 line was from Dr. Jaw-Ji Yang (Chung Shan Medical University, Taiwan).

siRNA against human GADD153 (sc-35437) and scrambled siRNA (sc-37007) were purchased from Santa Cruz Biotechnology and were transfected into cells using Lipofectamine 2000 according to the manufacturer's protocol (Invitrogen, Carlsbad, CA, USA). For the autophagy experiment, HCT116 cells were transiently transfected with the pEGFP or pEGFP-LC3 construct (a generous gift from Dr. Tamotsu Yoshimori, Osaka University, Japan) using the jetPEI transfection reagent according to the manufacturer's protocol (Polyplus-Transfection SA, Illkirch, France).

Cell viability assays

Cells were seeded onto 96-well culture plates at 8×10^3 cells/well and permitted to adhere overnight at 37 °C. After incubation, the cells were treated with a 0.5 mg/ml solution of 3-(4,5-dimethylthiazolyl-2-yl)-2,5-diphenyltetrazolium bromide (MTT; 100 μl/well) for 2 h at 37 °C. The number of viable cells was determined by uptake and reduction of MTT, assayed at 570 nm using a microplate reader. All experiments were performed at least in triplicate on three separate occasions. Data are presented as means ± SD.

Colony formation assay

Two hundred cells were seeded onto a 6-cm dish and incubated in culture medium with various concentrations of flavokawain B for 10 days to allow colony formation. For the inhibitor experiments, cells were pretreated with individual inhibitors for 1 or 2 h before 10 μM flavokawain B exposure in the presence of inhibitors. After incubation for 10 days, colonies were fixed in 1.25% glutaraldehyde at room temperature for 30 min, rinsed with distilled water, and stained with

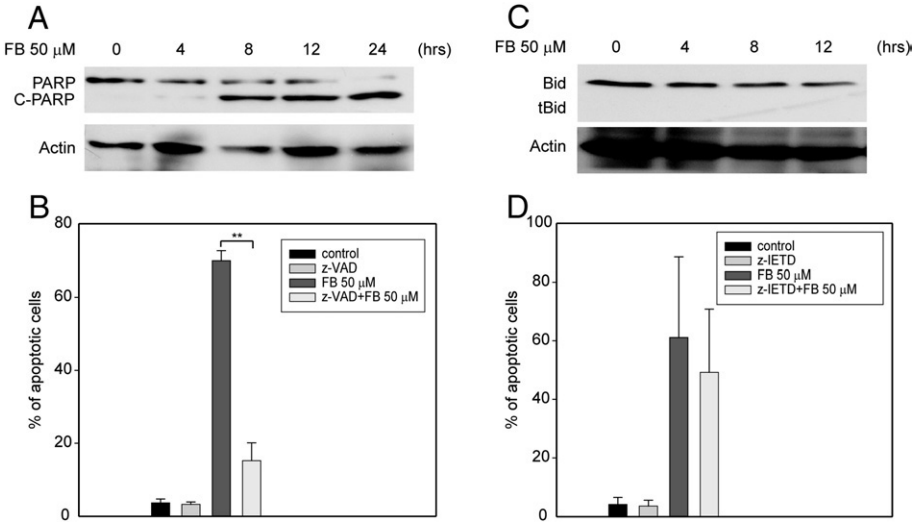

Fig. 2. Flavokawain B-induced caspase-dependent apoptosis. (A, C) HCT116 cells were treated with 50 μM flavokawain B for 0–24 h. Aliquots of cell lysates were separated by SDS–PAGE and analyzed for PARP (A) or Bid (C) protein expression by Western blotting as described under Materials and methods. β-Actin was used as an internal control to monitor for equal loading. (B, D) Cells were preincubated with or without 20 μM pancaspase inhibitor (z-VAD-fmk; B) or caspase-8 inhibitor (z-IETD-fmk; D) for 30 min, followed by treatment with 50 μM flavokawain B for 24 h. The percentage of apoptotic cells was determined by flow-cytometry analysis and the results are expressed as the percentage of total cells in early and late apoptotic populations (see Materials and methods). Values (means ± SE) are from at least three independent experiments. There was a significant difference in cells treated with z-VAD plus FB compared to the FB-only treatment group (**$p < 0.01$).

a 0.05% methylene blue solution. The number of colonies was counted and recorded.

Impedance measurement with the xCELLigence system

Cells (1×10^4/well) were seeded onto E-plates and incubated for 30 min at room temperature, followed by placing the E-plates onto the Real-Time Cell Analyzer station (xCELLigence system; Roche, Mannheim, Germany). Cells were grown for 24 h, with impedance measured every hour, before pretreatment with antioxidant for 1 h followed by addition of 10 μM flavokawain B. The cells were monitored every hour for a total of 80 h. In another experiment, 2×10^4/well GADD-knockdown and control cells were grown for 20 h before 10 μM flavokawain B exposure for a total of 80 h, with impedance measured every hour. Cell impedance is characterized by the cell index (CI) values ((Z_i-Z_0) ohm/15 ohm, where Z_0 is the background resistance and Z_i is the individual time point resistance) and the normalized cell index was determined as the CI_{ti} at a certain

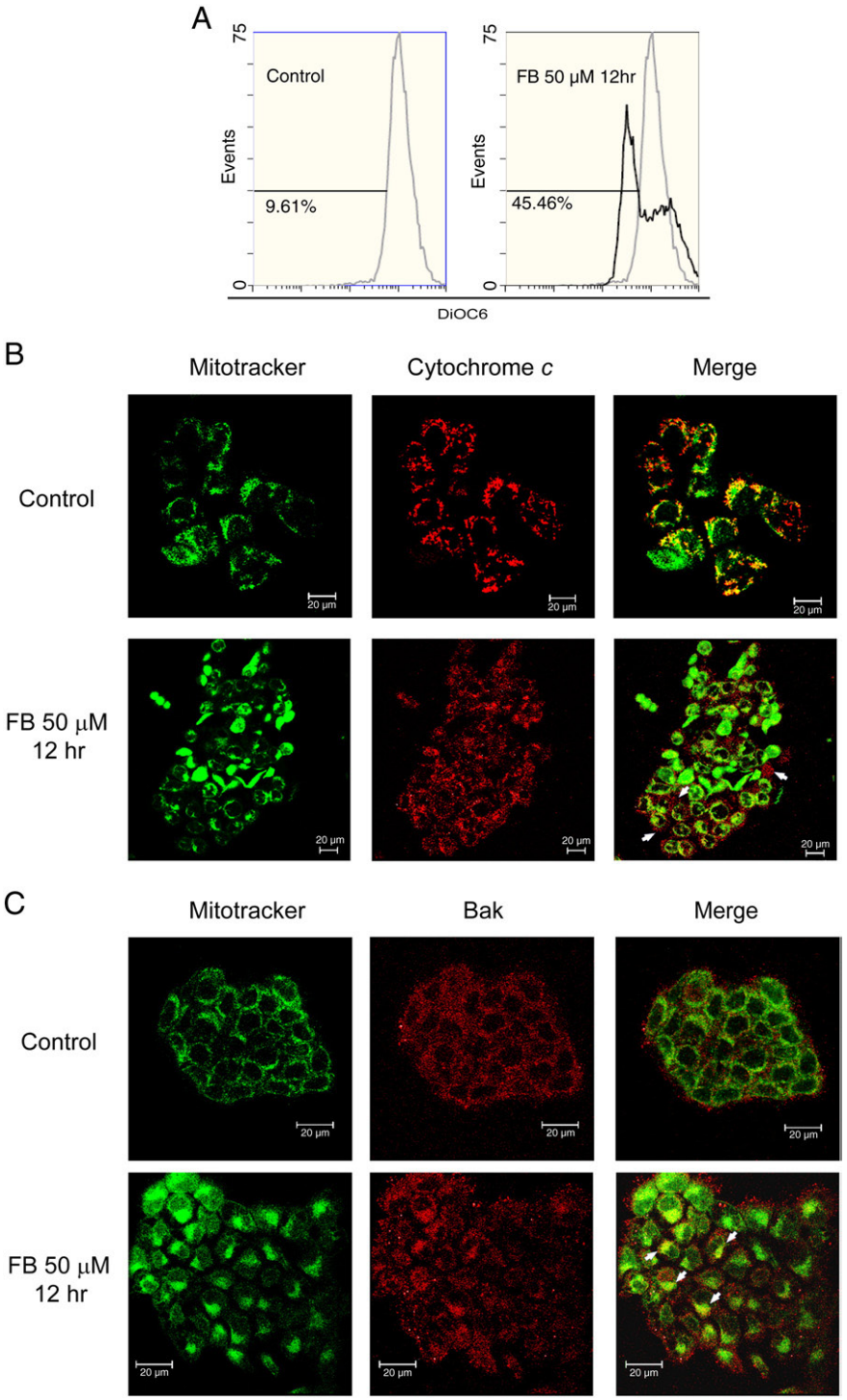

Fig. 3. Flavokawain B-induced mitochondria-dependent apoptosis. (A) The loss of mitochondrial membrane potential was assessed by flow cytometric analysis of $DiOC_6(3)$ retention in cells treated with FB for 12 h. (B, C) Representative images of laser confocal microscopic analyses of MitoTracker-stained mitochondria and cytochrome *c* (B) or Bak (C) subcellular localization in control and FB-treated cells are shown. The scale bars indicate 20 μm.

time point divided by the CI_{nml_time} at the normalization time point (nml_time).

Apoptosis assays

Apoptosis was measured using an annexin V–FITC apoptosis detection kit (BD PharMingen, San Jose, CA, USA). Cells cultured in 6-cm dishes were trypsinized and collected by centrifugation. The cell pellet was washed, resuspended in 1× binding buffer, and stained with annexin V–FITC, as recommended by the manufacturer. Cells were also stained with propidium iodide (PI) to detect necrosis or late apoptosis. The distribution of viable (FITC/PI-negative), early apoptotic (FITC-positive), late apoptotic (FITC/PI-double positive), and necrotic (PI-positive, FITC-negative) cells was analyzed using a Beckman Coulter FC500. The results are expressed as percentage of total cells.

Confocal microscopy

Cells were grown overnight on coverslips, treated with 50 μM flavokawain B for 12 h, and incubated with MitoTracker (Molecular Probes) for 20 min. Cells were then washed, fixed in 4% paraformaldehyde, washed with phosphate-buffered saline (PBS), and permeabilized with 0.01% Triton X-100. For the apoptosis experiments, coverslips were stained with anti-cytochrome *c* or anti-Bak antibodies before being observed under a microscope. Immunofluorescence images were acquired on a confocal microscope (TCS SP5; Leica Microsystems, Bannockburn, IL, USA).

Cytofluorimetric analysis of mitochondrial membrane potential

Changes in mitochondrial membrane potential characteristic of apoptosis were studied using the cationic lipophilic dye $DiOC_6(3)$. HCT116 cells were treated with 50 μM flavokawain B for 12 h. At the end of treatment, cells were washed and incubated with 40 nM $DiOC_6(3)$ for 30 min at 37 °C, followed by washing with PBS, after which the cell pellets were collected and resuspended in PBS. The fluorescence intensity of the cells was analyzed using a Beckman Coulter FC500.

Measurement of intracellular calcium concentrations

Free cytosolic calcium concentrations were measured using the cell-permeative, calcium ion-sensitive fluorescent dye Fluo-3AM. At the end of flavokawain B exposure for 1 h, cells were washed with PBS and incubated with 20 mM Fluo-3AM for 30 min. The cells were collected by trypsinization and centrifugation, washed with PBS, and centrifuged at 200 *g* for 5 min and intracellular calcium concentrations were analyzed using a Beckman Coulter FC500.

Measurement of ROS

At the end of flavokawain B treatment, cells (2×10^5) were washed with PBS and incubated with 5 μM H_2DCFDA in dimethyl sulfoxide for 30 min. Cells were collected by trypsinization and centrifugation, washed with PBS, centrifuged at 200 *g* for 5 min, and analyzed immediately using a Beckman Coulter FC500 flow cytometer.

Cell-cycle analysis

In brief, 10^6 cells were collected and washed in PBS, slowly fixed in 75% ethanol, and kept at −20 °C for at least 1 h. The cell pellet was then washed again with PBS and centrifuged at 500 *g* for 5 min. The pellet was resuspended in 200 μl cold PBS and stained in the dark with PI solution (20 mM Tris, pH 8, 1 mM NaCl, 0.1% NP-40, 1.4 mg/ml

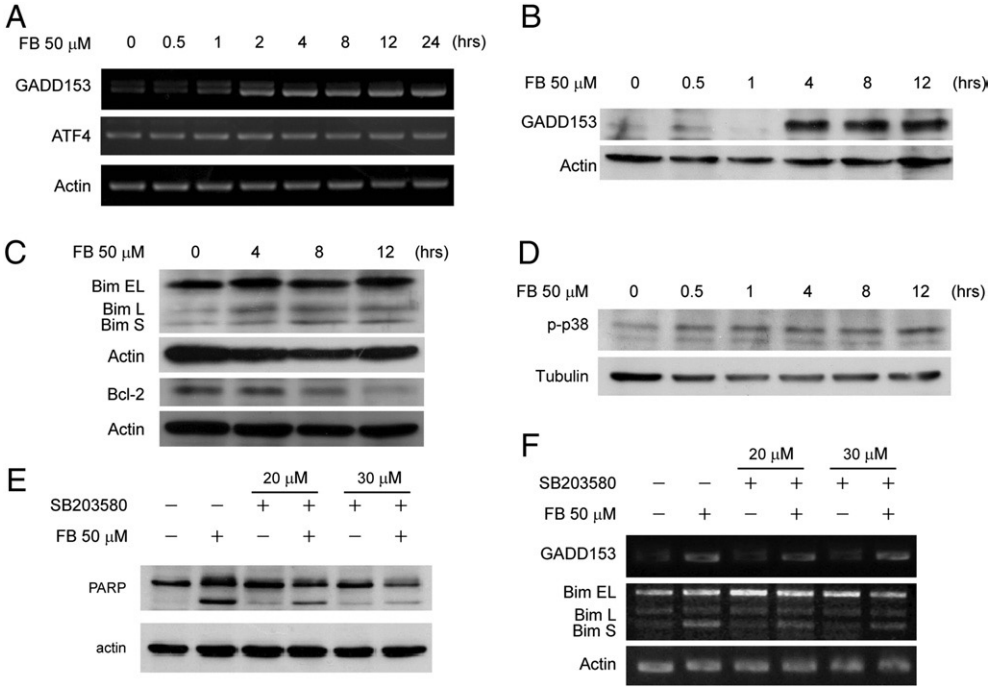

Fig. 4. Flavokawain B-induced GADD153 up-regulation. HCT116 cells were treated with 50 μM flavokawain B for 0–24 h. (A) GADD153 and ATF4 mRNA levels were determined by RT-PCR using β-actin as an internal control. (B, C, D) Cells were treated with 50 μM flavokawain B for 0–12 h. Aliquots of cell lysates were separated by SDS–PAGE and analyzed for GADD153 (B), Bim and Bcl-2 protein expression (C), or p38 phosphorylation (D) by Western blotting. β-Actin or tubulin was used as an internal control to monitor for equal loading. (E, F) HCT116 cells were pretreated with SB203580 for 2 h followed by treatment with 50 μM flavokawain B for 12 h. Aliquots of cell lysates were separated by SDS–PAGE and analyzed for PARP by Western blotting analysis. β-Actin was used as an internal control to monitor for equal loading (E). GADD153 and Bim mRNA levels were determined by RT-PCR using β-actin as an internal control (F).

RNase A, 0.05 mg/ml PI) for 30 min in ice. The total cellular DNA content was analyzed with a Beckman Coulter FC500.

Western blot analysis

Cell extracts were prepared in lysis buffer (20 mM Tris–HCl, pH 7.4, 100 mM NaCl, 5 mM EDTA, 2 mM phenylmethylsulfonyl fluoride, 10 ng/ml leupeptin, and 10 μg/ml aprotinin). Volumes of extract containing equal amounts of proteins (40 μg) were separated by SDS–PAGE and transferred onto nitrocellulose membranes (Schleicher & Schuell, Keene, NH, USA). The membranes were blocked, washed, and then probed with primary antibody. After being washed to remove primary antibody, the membranes were incubated with horseradish peroxidase-conjugated secondary antibody for 1 h. The blots were washed again and developed using enhanced chemiluminescence according to the manufacturer's protocol (Amersham Biosciences, Piscataway, NJ, USA).

Reverse transcriptase-polymerase chain reaction (RT-PCR)

Total RNA from HCT116 cells was isolated using the TRIzol reagent (Gibco). The first-strand cDNA was synthesized from 1 μg of total RNA using Superscript II (Life Technologies, Rockville, MD, USA). The sequences of the primers used to amplify GADD153 were 5′-AGTCATTGCCTTTCTCTTCG (sense) and 5′-GGTGCAGATTCACCATTCGG (antisense), those for ATF4 were 5′-TCAAACCTCATGGGTTCTCC (sense) and 5′-GTGTCATCCAACGTGGTCAG (antisense), those for Bim were 5′-TGATGTAAGTTCTGAGTGTG (sense) and 5′-CGCATATCTG-CAGGTTCAGCC (antisense), and those for β-actin were 5′-GATGAT-GATATCGCCGCGCT (sense) and 5′-TGGGTCATCTTCTCGCGGTT (antisense). Reaction conditions consisted of 30 cycles of 95 °C for 1 min, 58 °C for 1 min, and 72 °C for 1 min, followed by a final extension at 72 °C for 7 min. PCR products were analyzed by electrophoresis in 0.8% agarose gels.

Statistics

Data are expressed as the means ± SD of three independent experiments. The differences between the control and the treatment groups were calculated by one-way ANOVA, and a post hoc Dunnett test was used to evaluate significance levels.

Results

Flavokawain B effectively reduces viability and proliferation of colon cancer cells

The predominant chalcone from kava extract, flavokawain A, has been reported to induce apoptosis in bladder cancer cells through a Bax- and mitochondria-dependent pathway [11]. In this study, a structurally related compound, flavokawain B, was isolated from the rhizome of *A. pricei* and used in a cytotoxicity study. To determine an effective concentration range, we first tested the dose dependence of flavokawain B cytotoxicity in four cell lines, HCT116, A-549, NIH3T3, and HFW, measuring cell viability by MTT assays. Flavokawain B was significantly cytotoxic at concentrations of 25 μM and higher in all cells tested for 24 h (Fig. 1A) and, at 25 μM, induced a time-dependent decrease in viability of all four lines tested (Fig. 1B). This time-dependent cytotoxicity was especially prominent in the HCT116 colon cancer cell line compared to the others, including two noncancerous lines (NIH3T3 and HFW), and HCT116 cells were selected for use in subsequent studies. We also examined the toxicity of the structurally similar oxymethyl-substituted compound FB-OMe (2′,4′,6′-tri-methoxy chalcone) and found that this compound had no effect on cell viability (Fig. 1C), but how OMe replacement blunted the cytotoxicity of flavokawain B is not yet clear. Moreover, flavokawain B dramatically inhibited the colony-forming ability of HCT116 cells, reducing colony numbers to 51 and 5% of control at 10 and 25 μM, respectively, indicating a potent antiproliferative activity against colon cancer cells (Fig. 1D). In agreement with the viability results observed in Fig. 1B, flavokawain B was much less effective on the colony-forming ability of the other three lines, especially on that of human fibroblast (HFW) cells (Fig. 1D).

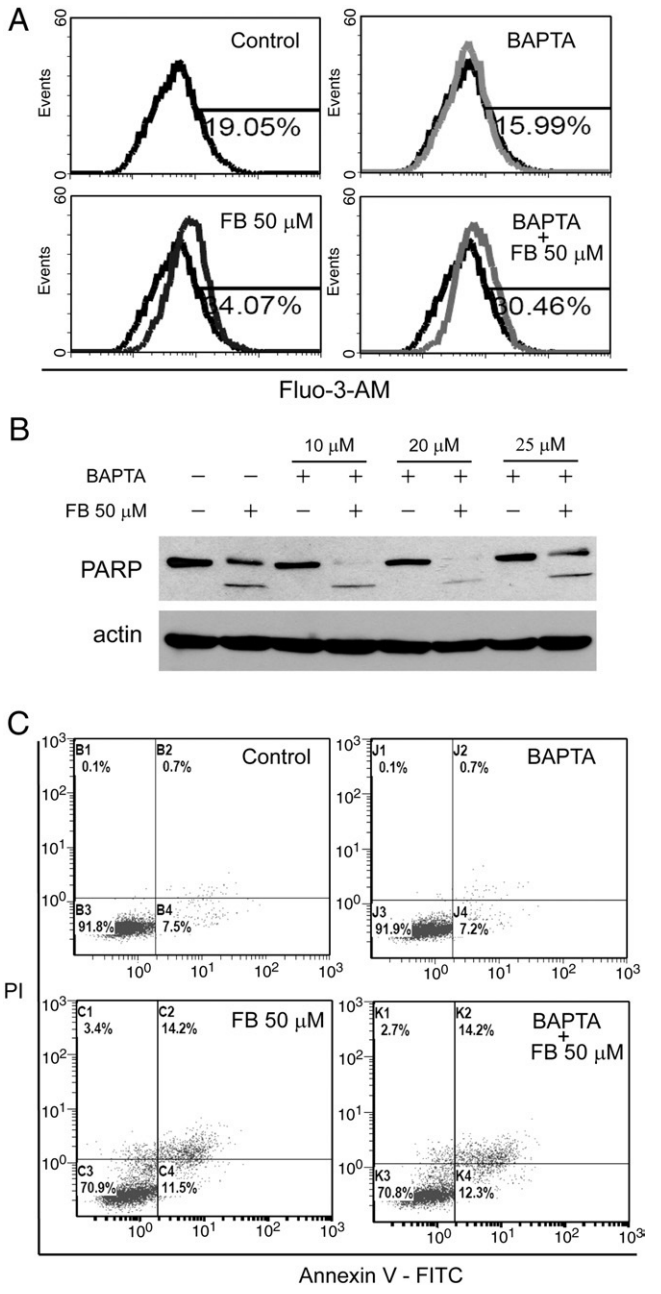

Fig. 5. Flavokawain-induced intracellular calcium level and the effect of calcium chelator on flavokawain B-induced apoptosis. HCT116 cells were preincubated with or without 10 μM (or higher) BAPTA for 20 min followed by treatment with 50 μM flavokawain B for 12 h. (A) Intracellular calcium concentration was analyzed by flow cytometry. Fluo-3AM fluorescence histograms show the overlay of control and FB-treated cells. The experiments were performed at least three times with similar results. (B) Aliquots of cell lysates were separated by SDS–PAGE and analyzed for PARP cleavage by Western blotting. β-Actin was used as an internal control to monitor for equal loading. (C) The distribution of viable, early apoptotic, later apoptotic, and necrotic cells was analyzed. The graphs depict apoptotic and necrotic populations of cells double stained with PI- and FITC-labeled annexin V. The results are expressed as percentage of total cells.

Flavokawain B triggers caspase- and mitochondria-dependent apoptosis

To further analyze the inhibitory effect of flavokawain B, we analyzed PARP cleavage and found that PARP cleavage was induced notably in cells treated with 50 μM flavokawain B for 8 h (Fig. 2A). In agreement with our PARP cleavage data, the percentage of apoptotic HCT116 cells was increased to nearly 70% in cells treated with 50 μM flavokawain B for 24 h, an effect that was considerably blunted by pretreatment with the pancaspase inhibitor z-VAD-fmk (Fig. 2B). To investigate whether the extrinsic pathway plays a role in flavokawain B-mediated apoptosis, we analyzed cells for the appearance of truncated Bid (tBid) and found that tBid was not induced by flavokawain B treatment (Fig. 2C). This observation was further supported by the results of experiments using the caspase-8 inhibitor Z-IETD-fmk, which was largely incapable of protecting against apoptosis (Fig. 2D), indicating that caspase-8 is dispensable in flavokawain B-mediated apoptosis.

We next examined the effect of flavokawain B on mitochondrial function in colon cancer cells. As illustrated in Fig. 3A, treatment of HCT116 cells with 50 μM flavokawain B induced a loss of mitochondrial membrane potential, measured by $DiOC_6(3)$ retention. In addition, treatment of HCT116 cells with flavokawain B increased the release of mitochondrial cytochrome *c* into the cytosol (indicated by arrows in Fig. 3B). This increased amount of cytosolic cytochrome *c* was associated with enhanced colocalization of Bak protein and mitochondria detected by MitoTracker staining (indicated by arrows in Fig. 3C). These results reveal that, in HCT116 cells, flavokawain B induced caspase- and mitochondria-dependent apoptosis, characterized by cytochrome *c* release and Bak translocation to mitochondria.

Flavokawain B enhances up-regulation and transcriptional activity of GADD153

To expand on our observations, we sought to identify upstream signals that mediate mitochondria-dependent apoptosis in our system. Because the ER plays major roles in the initiation of apoptosis, we examined the expression of GADD153, a marker for endoplasmic reticulum stress [20]. We found that GADD153 was notably up-regulated at the transcriptional level within 2 h of treating with 50 μM flavokawain B, an increase that was maintained for 24 h (Fig. 4A). The expression of GADD153 and apoptosis were shown to be regulated by enhanced transcription levels of ATF4 in response to proteasome inhibition [33]. However, we did not observe a significant increase in ATF4 RNA level (Fig. 4A). The increase in GADD153 mRNA was associated with a concomitant increase in GADD153 protein expression that was evident at 4 h of treatment (Fig. 4B).

GADD153, acting as a transcription factor in response to ER stress, is known to regulate the expression of a set of genes including many Bcl-2 family proteins to elicit mitochondrial cell death [21,28,29]. To demonstrate that the GADD153 induced by flavokawain B possesses transcriptional activity, we examined the expression of the GADD153 target genes Bcl-2 and Bim. Consistent with its apoptosis-inducing activity, flavokawain B reduced the expression of prosurvival Bcl-2 and augmented the expression of proapoptotic Bim, especially Bim L and Bim S (Fig. 4C). Phosphorylation of GADD153 by members of the p38 MAPK family is known to enhance GADD153 transcriptional activity [34,35]. In addition, p38 MAPK is documented to be important in IL-24-mediated induction of the GADD family and selective apoptosis [36]. Similarly, increased expression of GADD members by peroxynitrite is linked to the p38 MAPK pathway [37]. To study the role of p38 MAPK in our system, we analyzed the phosphorylation level of p38 MAPK and found that treatment with flavokawain B for 30 min induced phosphorylation of p38 MAPK (Fig. 4D). Pretreatment with the p38 MAPK inhibitor SB203580 significantly decreased the flavokawain-induced PARP cleavage (Fig. 4E) as well as the transcriptional level of the Bim short form that was stimulated by flavokawain B (Fig. 4F). In addition, we also observed an inhibition of flavokawain B-induced GADD153 RNA level by the p38 MAPK inhibitor (Fig. 4F). These changes in the protein and RNA levels of GADD153 target genes are consistent with up-regulation of GADD153

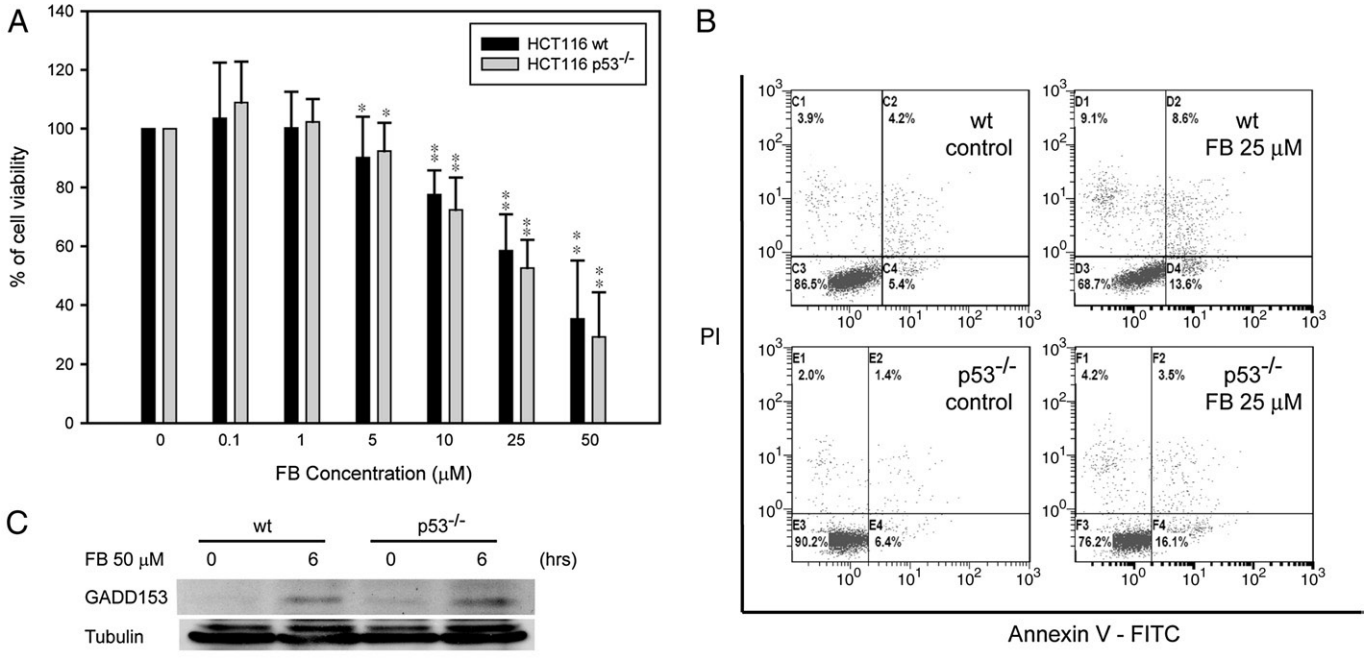

Fig. 6. The cytotoxic effect of flavokawain B was independent of p53. (A) HCT116 p53 wild-type and p53-null cells were exposed to various concentrations of flavokawain B for 24 h, and cell viability was measured using MTT assays. Values (means ± SE) are from at least three independent experiments. There was a significant decrease in cell viability in cells treated with flavokawain B compared with controls (*$p<0.05$, **$p<0.01$). (B) p53 wild-type and p53-null cells were treated with or without 25 μM flavokawain B for 24 h, and the distribution of viable, early apoptotic, later apoptotic, and necrotic cells was analyzed. The graphs depict apoptotic and necrotic populations of cells double stained with PI- and FITC-labeled annexin V. The results are expressed as percentage of total cells. (C) p53 wild-type and p53-null cells were treated with 50 μM flavokawain B for 0–6 h. Aliquots of cell lysates were separated by SDS–PAGE and analyzed for GADD153 level by Western blotting. Tubulin was used as an internal control to monitor for equal loading.

expression and increased phosphorylation of p38 MAPK to enhance transcriptional activity of GADD153.

Because calcium signaling plays a vital role in ER-mediated apoptosis [38], we further analyzed the intracellular calcium concentration in treated cells. As shown in Fig. 5A, flavokawain B treatment for 1 h increased intracellular calcium levels. However, pretreatment with 10 μM BAPTA, a common chelator of intracellular calcium ions, did not effectively attenuate flavokawain B-induced intracellular calcium levels (Fig. 5A). Similarly, the chelator was ineffective at reducing flavokawain B-mediated PARP cleavage (Fig. 5B) as well as protecting cells against apoptosis (Fig. 5C). However, pretreatment with high concentrations (>10 μM) of BAPTA alone induced intracellular calcium concentration in our system. It is not yet clear whether calcium signaling plays a key role in flavokawain B-induced apoptosis. Further experiments are crucial to clarify this issue.

Flavokawain B-induced up-regulation of GADD153 and apoptosis are independent of p53

Liu et al. have reported a p53-dependent up-regulation of GADD153 and apoptosis upon hypoxia in HCT116 cells [39]. To examine whether p53 is important in flavokawain B-mediated apoptosis, we conducted experiments using a p53-null HCT116 line. Flavokawain B reduced cell viability to similar extents in both wild-type p53-containing and p53-null HCT116 cell lines (Fig. 6A). Consistent with this, the percentages of apoptotic cells were comparable in flavokawain B-treated p53 wild-type and p53-null lines (Fig. 6B). Most importantly, treatment of p53-null cells with 50 μM flavokawain B for 6 h stimulated GADD153 expression, verifying that the induction of apoptosis and GADD153 expression by flavokawain B was independent of p53 (Fig. 6C).

The generation of reactive oxygen species is required for flavokawain B-induced apoptosis

GADD153 has been shown to down-regulate Bcl-2, exhaust cellular glutathione, and enhance ROS production, resulting in apoptosis [28]. Other evidence, however, suggests that ROS lie upstream of ER stress in the pathway leading to apoptosis [40–42]. To clarify the role of intracellular ROS generation in flavokawain B-induced apoptosis, we utilized the fluorescent dye H_2DCFDA, which produces enhanced fluorescence when cells generate ROS. In cells treated with flavokawain B, intracellular ROS production increased at 30 min (Fig. 7A). This increase in H_2DCFDA-based fluorescence was inhibited by pretreatment with the ROS scavenger *N*-acetylcysteine (NAC), which reduced the flavokawain B-induced increase in fluorescence from 44.1 to 7.9% (Fig. 7B). We also validated that the apoptotic effect of flavokawain B treatment for 6 h was inhibited by pretreatment with NAC (Fig. 7C). NAC pretreatment also completely abrogated the up-regulation of GADD153 and concurrent cleavage of PARP induced by flavokawain B (Figs. 7D and E). These results indicate that ROS generation is required for flavokawain B-induced GADD153 expression and apoptosis.

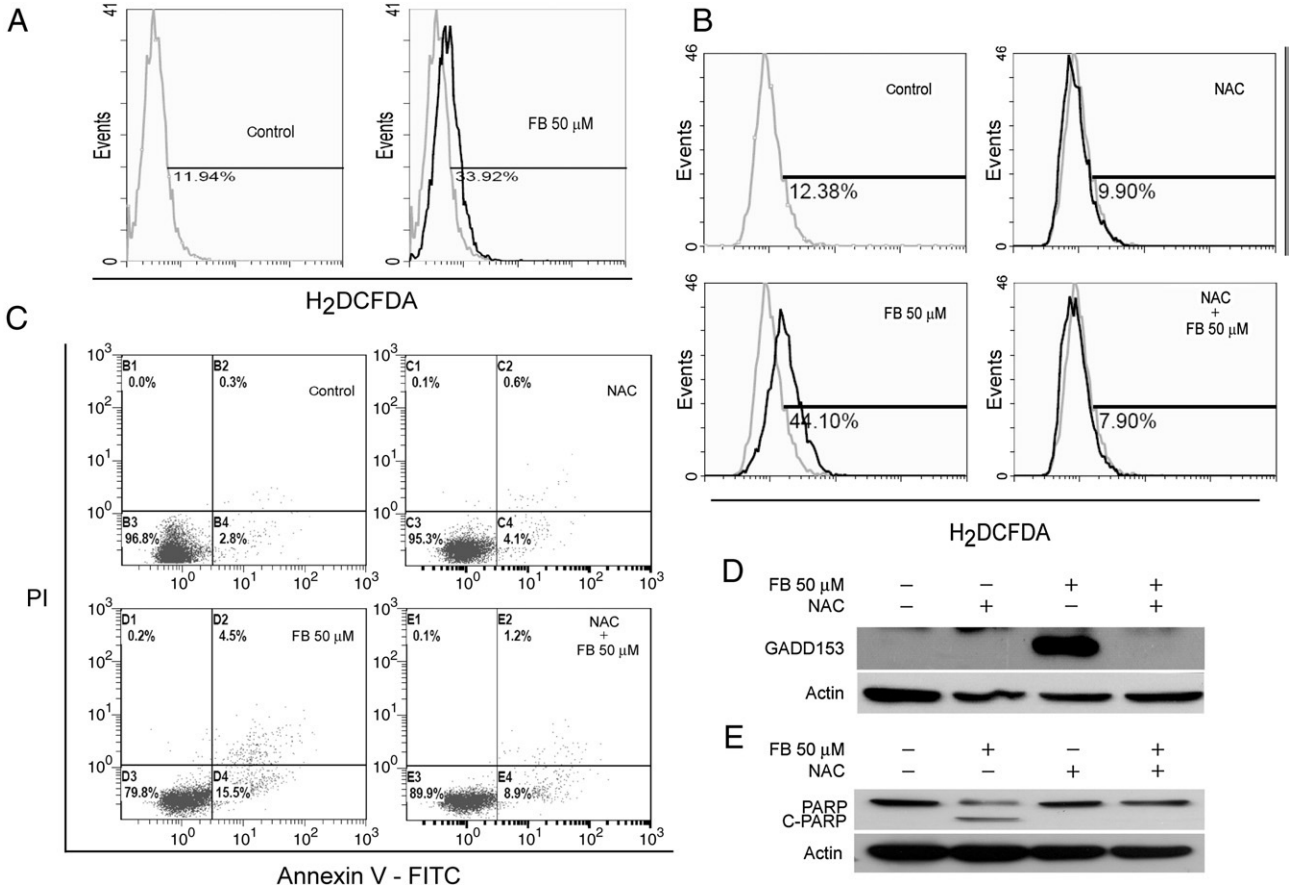

Fig. 7. Flavokawain B-induced intracellular ROS generation, resulting in apoptosis. (A) Percentage changes in intracellular ROS generation were measured in HCT116 cells treated with or without 50 μM flavokawain B for 30 min. (B, C) HCT116 cells were preincubated with or without 20 mM NAC at 37 °C for 2 h before exposure to 50 μM flavokawain B for 6 h. Percentage changes in intracellular ROS generation were measured (B). The distribution of viable, early apoptotic, later apoptotic, and necrotic cells was analyzed (C). The graphs depict apoptotic and necrotic populations of cells double stained with PI- and FITC-labeled annexin V. The results are expressed as percentage of total cells. (D, E) Cells were preincubated with or without 20 mM NAC for 2 h before exposure to 50 μM flavokawain B for 6 h. Aliquots of cell lysates were separated by SDS–PAGE and analyzed for GADD153 (D) and PARP cleavage (E). Anti-β-actin was used as a loading control. The graphs are representative of three independent experiments.

To investigate the role of GADD153 in flavokawain B-induced apoptosis, we used the RNAi technique to knock down the induction of GADD153 in HCT116 cells. The up-regulation of GADD153 by flavokawain B was effectively inhibited at both protein (Fig. 8A) and mRNA levels (Fig. 8B). Moreover, GADD153 knockdown markedly reduced the flavokawain B-enhanced mRNA level of short-form Bim (Fig. 8B). Using flow cytometry to assess cell death, we found that GADD153 down-regulation diminished flavokawain B-induced apoptosis; as an alternative, cells die of necrosis (Fig. 8C). Furthermore, the xCELLigence system was used to continuously monitor the effect of flavokawain B on cellular events in GADD153-knockdown cells, measuring electrical impedance and displaying the CI value. The presence of the cells on the top of the electrodes produces an elevation in electrode impedance that is determined by the cell number and the degree of cell adhesion. We showed that untreated wild-type cells demonstrated an increase in the cell index values and reached a plateau phase after 70 h. RNAi-transfected cells exhibited a slower growth rate compared to the wild type, especially the GADD153-knockdown line. After the point of treatment, cells displayed a decreased cell index pattern induced by flavokawain B

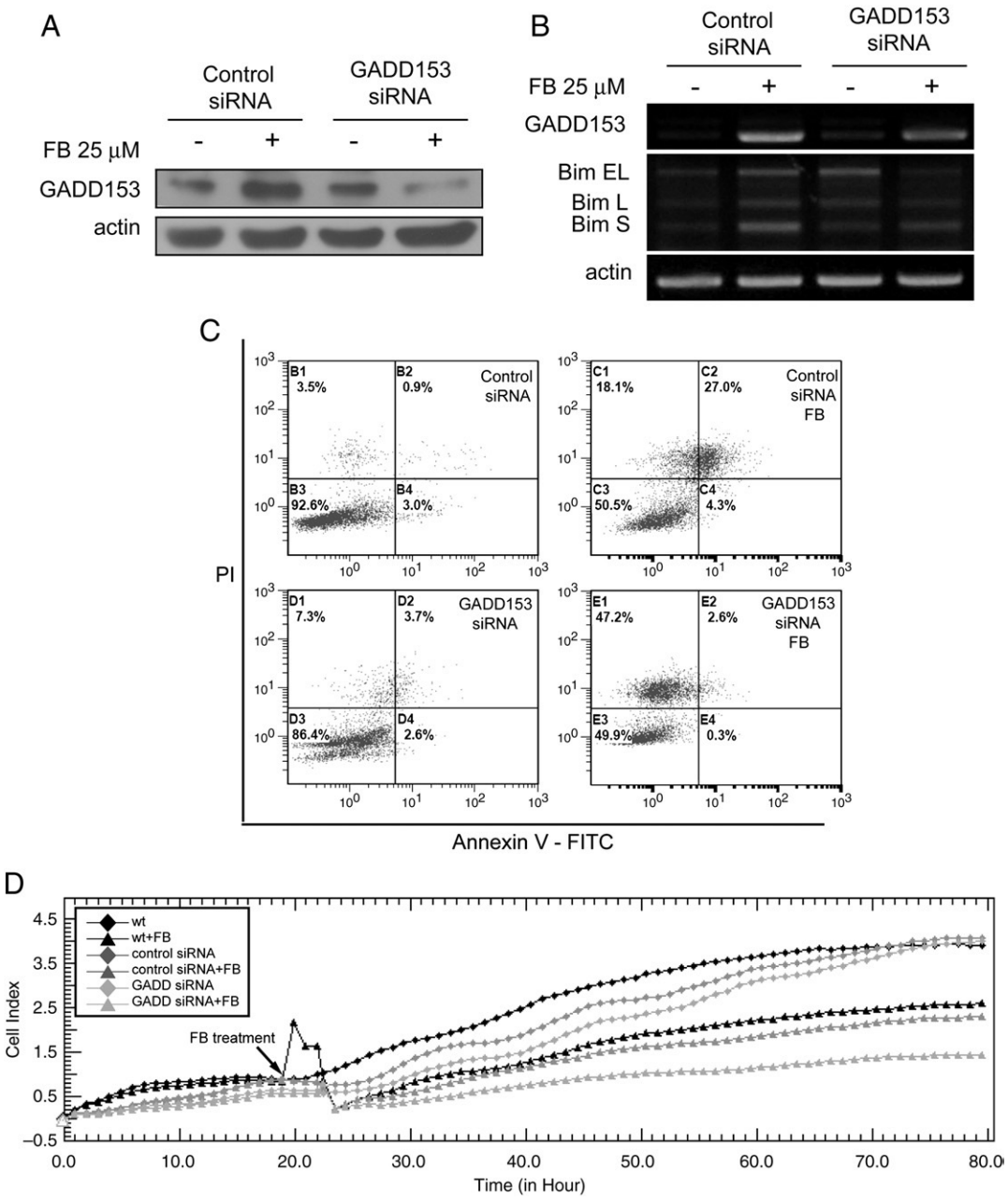

Fig. 8. GADD153 knockdown reduced flavokawain B-induced protein expression, mRNA level, and apoptosis. HCT116 cells were transfected with control siRNA or GADD153 siRNA as described under Materials and methods. Cells were treated with or without 25 μM flavokawain B for 12 h. (A) Aliquots of cell lysates were separated by SDS–PAGE and analyzed for GADD153 level by Western blotting. β-Actin was used as an internal control to monitor for equal loading. (B) GADD153 and Bim mRNA levels were determined by RT-PCR using β-actin as an internal control. (C) Cells were assayed for apoptosis. The graphs depict apoptotic and necrotic populations of cells double stained with PI- and FITC-labeled annexin V. The results are expressed as percentage of total cells. (D) Dynamic monitoring of cells treated with or without 10 μM flavokawain B using impedance technology as described under Materials and methods. Normalized cell index was measured over 80 h.

in all three lines. Importantly, GADD153 knockdown did not reverse flavokawain B-repressed cell growth and the cells displayed the slowest growth compared to wild-type and control RNAi cells (Fig. 8E). Similarly, there was no protective effect of GADD153 knockdown on flavokawain B-induced clonogenic cell killing (data not shown). These data suggest a key role for GADD153 in flavokawain B-induced apoptosis but not cell growth inhibition.

Multiple pathways are activated by flavokawain B leading to cell growth reduction

To further analyze whether the flavokawain B-mediated growth inhibition resulted from impaired cell proliferation, the cell-cycle profile was examined by nuclear DNA staining with propidium iodide using flow cytometry. The percentage of G2/M cells notably increased

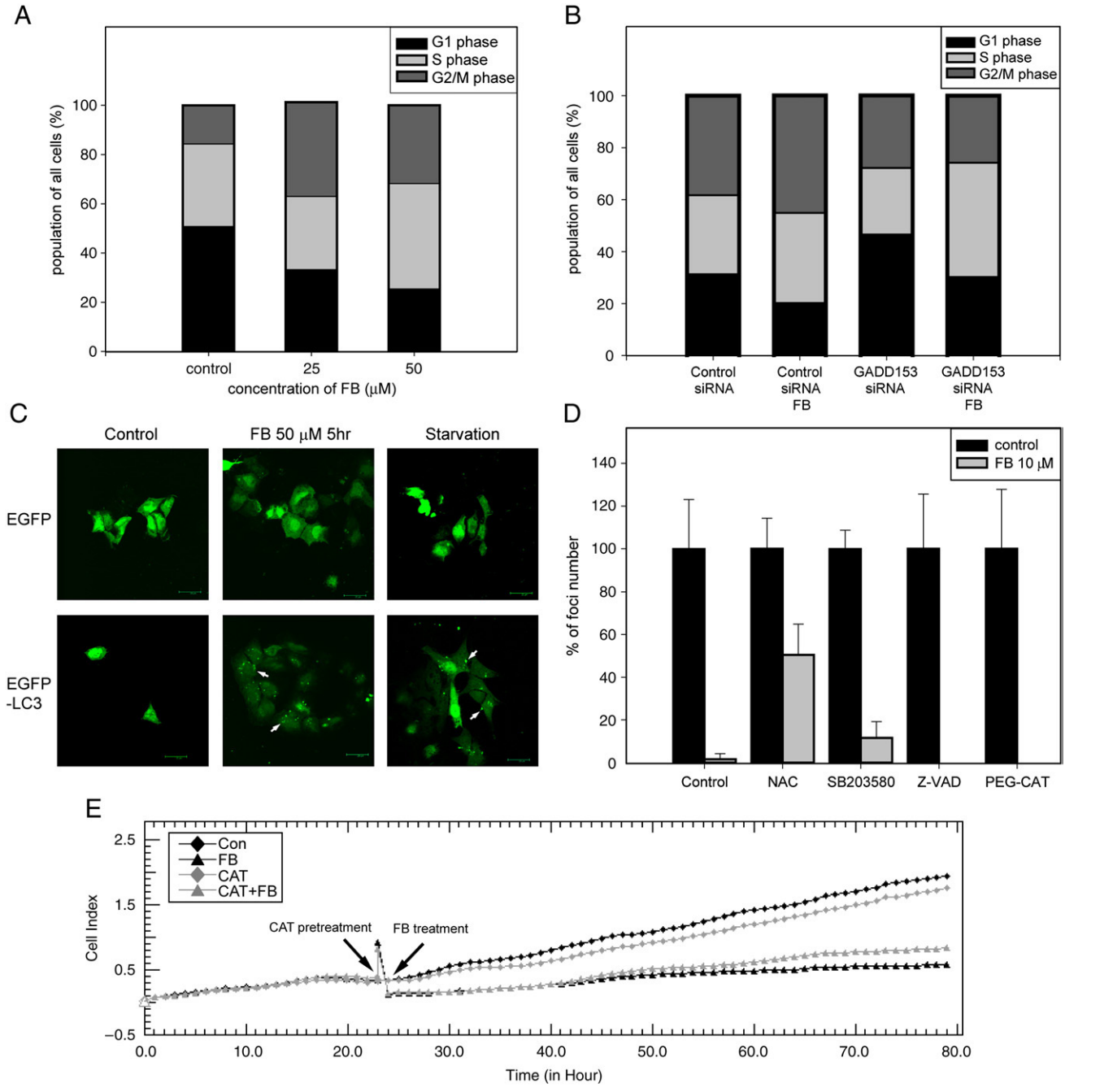

Fig. 9. Effect of flavokawain B on G2 accumulation, autophagy, colony-forming ability, and cell impedance measurement. (A) HCT116 cells were treated with or without flavokawain B for 12 h and assayed for cell-cycle phase. The graph is representative of three independent experiments. (B) HCT116 cells were transfected with control siRNA or GADD153 siRNA as described under Materials and methods. Cells were then treated with or without 25 μM flavokawain B for 12 h and assayed for cell-cycle phase. The graph is representative of three independent experiments. (C) Forty-eight hours after transfection with expression plasmids for EGFP or EGFP–LC3 fusion protein, HCT116 cells were treated with 50 μM flavokawain B or serum-starved for 5 h and analyzed by fluorescence microscopy for LC3 distribution. Representative images are shown. (D) Cells seeded at 200 cells per dish were pretreated with 20 mM NAC for 2 h, 25 μM SB203580 for 2 h, 25 μM z-VAD for 2 h, or 200 U/ml PEG–CAT for 1 h before 10 μM flavokawain B treatment for 10 days in the presence of individual inhibitors. Cells were allowed to form colonies and colony numbers were counted and recorded. Values (means ± SE) are from three independent experiments. (E) Dynamic monitoring of the effect of PEG–CAT pretreatment on flavokawain B-inhibited HCT116 cell growth using impedance technology as described under Materials and methods. Cells were pretreated with 200 U/ml PEG–CAT for 1 h before 10 μM flavokawain B treatment for another 60 h in the presence of antioxidant. Normalized cell index was measured over 80 h.

with flavokawain B treatment in HCT116 cells (Fig. 9A), whereas GADD153 knockdown reversed flavokawain B-induced G2/M accumulation (Fig. 9B). Moreover, flavokawain B-treated cells exhibited changes in LC3 distribution indicative of the formation of autophagic vacuoles. In these cells, the pattern of EGFP–LC3 localization was similar to that observed in cells serum-starved for 5 h, a standard procedure for inducing autophagy (Fig. 9C). Based on these results, it is possible to propose that flavokawain B induces multiple pathways leading to HCT116 cell growth inhibition in addition to apoptosis.

To confirm this interpretation, we tested the effects of individual inhibitors on flavokawain B-repressed colony-forming ability after 10-day exposure. It was found that pretreatment with NAC (a ROS scavenger) for 2 h before treatment diminished flavokawain B-induced clonogenic cell killing effectively (Fig. 9D). A similar result was observed in cells pretreated with SB203580 (a p38 MAPK inhibitor), although to a lesser extent. Pretreatment with z-VAD-fmk (pancaspase inhibitor) or PEG–CAT (catalase, which degrades hydrogen peroxide), however, did not confer protection against flavokawain B toxicity (Fig. 9D). Pretreatment with DPI (a pan-NADPH oxidase inhibitor) was also ineffective at reducing flavokawain B-mediated clonogenic cell killing (data not shown). Additionally, cell impedance measurements showed that pretreatment with PEG–CAT before flavokawain B exposure augmented the flavokawain B-reduced cell index values moderately, suggesting that this antioxidant shielded cells from flavokawain B-derived ROS damage (Fig. 9E). However, the pretreatment with NAC seemed to interfere with the cell impedance measurement; therefore, no data were obtained. These results indicate that, in HCT116 cells, certain ROS derived from flavokawain B are important in cell growth inhibition.

Taken together, our results reveal that flavokawain B is markedly cytotoxic to HCT116 cells and acts through multiple pathways, including G2/M accumulation, autophagy, and apoptosis. Primarily, in this study, we demonstrate that flavokawain B provokes intracellular ROS generation, p38 MAPK phosphorylation, and GADD153 up-regulation, leading to mitochondria-dependent apoptosis in human colon cancer cells.

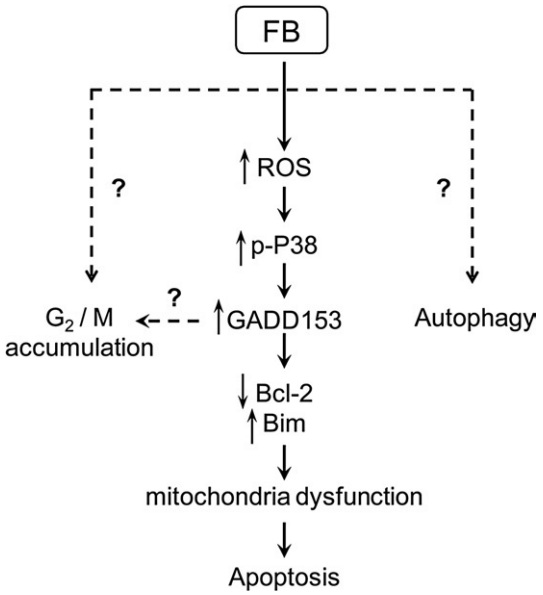

Fig. 10. Schematic diagram of flavokawain B-mediated cytotoxicity.

Discussion

In this study, we investigated the antiproliferative effect of flavokawain B, isolated from rhizome extracts of *A. pricei* Hayata, on colon cancer cells. Our results provide the first evidence for cytotoxicity mediated by flavokawain B through the induction of G2/M accumulation, autophagy, and apoptosis, leading to HCT116 colon cancer cell growth inhibition. In particular, flavokawain B provokes apoptosis, demonstrating that this chalcone enhances intracellular ROS generation, p38 MAPK phosphorylation, and GADD153 expression. GADD153, in turn, regulates the protein levels of Bcl-2 family members, causing a loss of mitochondrial membrane potential and apoptosis in HCT116 cells (summarized in Fig. 10).

Naturally occurring chalcones are precursor compounds for flavonoid synthesis in plants that have documented potential as therapeutic agents against cancer cells, reflecting their effects on cell-cycle progression, ROS production, and apoptosis [5,43,44]. Primarily, flavokawain A, the predominant chalcone in kava extracts, induces Bax- and mitochondria-dependent apoptosis and cell-cycle arrest in bladder cancer cells [11,45]. Interestingly, extracts of *A. pricei* Hayata, a perennial plant native to Taiwan commonly used in traditional Chinese food and folk medicine, have been documented to have anticancer properties in human carcinoma KB cells that are associated with induction of the mitochondria-dependent apoptotic pathway [46]. Furthermore, a recent study has focused on the anti-inflammatory effect of *A. pricei* Hayata [47]. Unexpectedly, we isolated for the first time a novel flavokawain B from *A. pricei* Hayata. Using the Bax-dependent apoptotic activity of the structurally related flavokawain A in cancer cells as a guide [11], we further studied the biological activity of this novel compound. Our cell viability assay revealed that flavokawain B induced cytotoxicity in a concentration- and time-dependent manner; remarkably, HCT116 cells exhibited a higher sensitivity to the anticancer effects of flavokawain B than did all other lines tested. Consistent with this result, flavokawain B specifically induced clonogenic cell killing in HCT116 cells, whereas it was much less effective in others, including two noncancerous lines (Fig. 1). There is precedence for the preferential inhibition of cancer cells by botanicals [48,49], a notion that is supported by this study. Although current understanding regarding their cytotoxic role in cancer cells is not entirely clear, a possible explanation may reside in a distinctive pathway in cancer cells that is currently under investigation in our laboratory.

Further exploration of the inhibitory effects of flavokawain B in HCT116 cells provided several lines of evidence to support a role for the intrinsic apoptosis pathway, including loss of mitochondrial membrane potential, Bak translocation, release of cytochrome *c* into the cytosol, and PARP cleavage (Figs. 2 and 3). These observations are not surprising because several laboratories have described mitochondria-dependent pathways in the cytotoxicity of various flavonoids [50–52]. Hence, the ultimate goal of this study was to identify the signaling elements upstream of mitochondria that are involved in flavokawain B-induced apoptosis. We approached this problem using the caspase-8 inhibitor z-IETD-fmk, which has been used in numerous studies to support a role for caspase-8 in the extrinsic pathway in flavonoid-mediated apoptosis [53,54]. We found that there was no appearance of truncated Bid and that pretreatment with z-IETD-fmk did not shield cells from apoptosis induced by flavokawain B, implying that the extrinsic apoptotic pathway plays a much less important role in our system (Fig. 2).

An exciting finding of this study is that flavokawain B elevates GADD153 protein expression and results in altered levels of Bcl-2 family members. Western blot and RT-PCR analyses revealed an up-regulation of GADD153 at both mRNA and protein levels (Figs. 4A and B). Elevated GADD153 is associated with various stresses—in particular, stresses in the ER, where protein synthesis, assembly, folding, and modification take place. Any such disturbance in the ER can lead to the accumulation of unfolded proteins and cause an ER stress response [18]. There is a growing awareness that apoptosis initiated by ER stress can cause mitochondrial damage [23,24]. However, the link between ER stress and the intrinsic apoptotic pathway has remained ambiguous. One suggested mechanism is that augmented GADD153 activity results in down-regulation of Bcl-2 and disruption of cellular redox homeostasis,

leading to ER stress-mediated apoptosis [28]. To verify that elevated GADD153 expression induced by flavokawain B is associated with increased transcriptional activity, we analyzed the expression of proteins encoded by the GADD153 target genes Bcl-2 and Bim of the Bcl-2 family [28,29]. Proapoptotic Bim was significantly up-regulated by flavokawain B concurrent with down-regulation of antiapoptotic Bcl-2 expression, changes that were associated with mitochondria dysfunction (Figs. 4C and 3). Three isoforms of Bim protein generated by alternative splicing are documented to be apoptotic, in particular the shortest one being the most effective [55]. In our system, expression of all three isoforms of Bim protein (Bim EL, Bim L, and Bim S) was up-regulated by flavokawain B (Fig. 4C). Moreover, we showed that an increase in p38 MAPK phosphorylation was induced by flavokawain B and pretreatment with a p38 MAPK inhibitor, SB203580, effectively reduced the PARP cleavage mediated by flavokawain B (Fig. 4E). The p38 MAPK inhibitor also notably reduced the transcriptional level of the Bim S form induced by flavokawain B, the most potent form to be apoptotic (Fig. 4F). Importantly, knockdown of GADD153 by RNA interference inhibits flavokawain B-induced mRNA levels of Bim S and apoptosis, indicating a crucial role for GADD153 in the apoptotic process triggered by flavokawain B (Fig. 8). Both gain-of-function and loss-of-function approaches have established a close link between GADD153 phosphorylation by p38 MAPK and GADD153 transcriptional activation [36,37], a connection that is reinforced by our findings in this study (Fig. 4). Although flavokawain B increased intracellular calcium concentrations, also a hallmark of ER stress-mediated apoptosis, pretreatment with a calcium chelator (BAPTA) did not alleviate flavokawain B-increased intracellular calcium levels, PARP cleavage, or apoptosis (Fig. 5). The close link between calcium signaling and ER stress-mediated apoptosis has been reported utilizing BAPTA as a chelator for intracellular calcium ions [38,56]. It is not yet clear, at this point, why BAPTA failed to reduce flavokawain B-induced intracellular calcium levels in our system. Further experiments are in progress to clarify this issue.

Consistent with previous reports, which have shown that flavonoids provoke oxidative stress [57,58], our results showed that flavokawain B also induced ROS generation. By pretreating cells with NAC, we demonstrated that ROS are essential for flavokawain B-induced GADD153 up-regulation and apoptosis (Fig. 7). Furthermore, NAC pretreatment effectively protects cells from flavokawain B-induced clonogenic cell killing (Fig. 9D), confirming that ROS derived from flavokawain B are essential in the pathway. A recent study has demonstrated that GADD153 is involved in ROS-mediated apoptosis in human acute promyelocytic leukemia NB4 cells, and siRNA-mediated GADD153 knockdown effectively reduces sodium selenite-induced apoptosis [40], a pathway that is reinforced in this study. Surprisingly, in addition to promoting apoptosis, flavokawain B was shown to clearly induce autophagy (Fig. 9C), a mechanism for degrading intracellular proteins that is also a form of programmed cell death. This mechanism has been previously observed in colon cancer cells treated with the flavonoid quercetin [59] or with anthocyanin extracts [60]. It is therefore of great interest to identify the molecular mechanisms by which flavokawain B triggers autophagy.

The results from our study demonstrate that flavokawain B might be a novel promising chemocytotoxic agent for treating colon cancer, a premise supported by our clonogenic cell-killing data (Fig. 1D). A recent report from Tang et al. [61] has shown that flavokawain B of kava extract triggers apoptosis in prostate cancer cells through increased expression of Bim and Puma. Similarly, Li et al. [62] suggest that flavokawain B is cytotoxic in human hepatoma HepG2 cells, although it also inhibits human normal liver L-02 cells with lower LC_{50}. In addition to cytotoxicity, the anti-inflammatory activity of flavokawain B has just been demonstrated [63], suggesting that this novel chalcone possesses multiple important bioactivities.

In conclusion, we report a previously unknown apoptotic property of flavokawain B, a novel chalcone isolated from *A. pricei* Hayata, in regulating oxidative stress, p38 MAPK signaling, GADD153 expression, and mitochondria function and promoting apoptosis in HCT116 colon cancer cells.

Acknowledgments

We thank Dr. Tamotsu Yoshimori (Osaka University, Japan) for his generous gift of the pEGFP-LC3 construct, Dr. Ping-Shan Lai for his technical support with confocal microscopy, Dr. Chia-Che Chang for providing wild-type and p53-null HCT116 cells, Dr. Show-Mei Chuang for the HFW and A549 cells, and Jun-Hong Xiao for the preparation of flavokawain B. This work was supported by grants from the National Science Council (NSC 97-2313-B-005-016-MY3) and the Ministry of Education, Taiwan, Republic of China, under the ATU plan.

References

[1] Johnson, J. J.; Mukhtar, H. Curcumin for chemoprevention of colon cancer. *Cancer Lett.* **55:**170–181; 2007.
[2] Raja, S. M.; Chen, S.; Yue, P.; Acker, T. M.; Lefkove, B.; Arbiser, J. L.; Khuri, F. R.; Sun, S. Y. The natural product honokiol preferentially inhibits cellular FLICE-inhibitory protein and augments death receptor-induced apoptosis. *Mol. Cancer Ther.* **7:** 2212–2223; 2008.
[3] Fedorov, S. N.; Shubina, L. K.; Bode, A. M.; Stonik, V. A.; Dong, Z. Dactylone inhibits epidermal growth factor-induced transformation and phenotype expression of human cancer cells and induced G1–S arrest and apoptosis. *Cancer Res.* **67:** 5914–5920; 2007.
[4] Wolf, I.; O'Kelly, J.; Wakimoto, N.; Nguyen, A.; Amblard, F.; Karlan, B. Y.; Arbiser, J. L.; Koeffler, H. P. Honokiol, a natural biphenyl, inhibits in vitro and in vivo growth of breast cancer through induction of apoptosis and cell cycle arrest. *Int. J. Oncol.* **30:** 1529–1537; 2007.
[5] Singh, R. P.; Agarwal, R. Natural flavonoids targeting deregulated cell cycle progression in cancer cells. *Curr. Drug Targets* **7:**345–354; 2006.
[6] Lorenzo, P.; Alvarez, R.; Oritz, M. A.; Alvarez, S.; Piedrafita, F. J.; de Lera, A. R. Inhibition of IkappaB kinase-beta and anticancer activities of novel chalcone adamantyl arotinoids. *J. Med. Chem.* **51:**5431–5440; 2008.
[7] Yun, J. M.; Kweon, M. H.; Kwon, H.; Huang, J. K.; Mukhtar, H. Induction of apoptosis and cell cycle arrest by a chalcone panduratin A isolated from Kaemferia pandurata in androgen-independent human prostate cancer cells PC3 and DU145. *Carcinogenesis* **27:**1454–1464; 2006.
[8] Go, M. L.; Wu, X.; Liu, X. L. Chalcones: an update on cytotoxic and chemoprotective properties. *Curr. Med. Chem.* **12:**481–499; 2005.
[9] Henderson, B. E.; Kolonel, L. N.; Dworsky, R.; Kerford, D.; Mori, E.; Singh, K.; Thevenot, H. Cancer incidence in the islands of the Pacific. *Natl. Cancer Inst. Monogr.* **69:**73–81; 1985.
[10] Steiner, G. G. The correlation between cancer incidence and kava consumption. *Hawaii Med. J.* **59:**420–422; 2000.
[11] Zi, X.; Simoneau, A. R. Flavokawain, a novel chalcone from kava extract, induces apoptosis in bladder cancer cells by involvement of Bax protein-dependent and mitochondria-dependent apoptotic pathways and suppresses tumor growth in mice. *Cancer Res.* **65:**3479–3486; 2005.
[12] Wajant, H. The Fas signaling pathway: more than a paradigm. *Science* **296:** 1635–1636; 2002.
[13] Er, E.; Oliver, L.; Cartron, P. F.; Juin, P.; Manon, S.; Vallette, F. M. Mitochondria as the target of the pro-apoptotic protein Bax. *Biochim. Biophys. Acta* **1757:** 1301–1311; 2006.
[14] Kuwana, T.; Mackey, M. R.; Perkins, G.; Ellisman, M. H.; Latterich, M.; Schneiter, R.; Green, D. R.; Newmeyer, D. D. Bid, Bax and lipids cooperate to form supramolecular openings in the outer mitochondrial membrane. *Cell* **111:** 331–342; 2002.
[15] Lee, H. J.; Wang, C. J.; Kuo, H. C.; Chou, F. P.; Jean, L. F.; Tseng, T. H. Induction apoptosis of luteolin in human hepatoma HepG2 cells involving mitochondria translocation of Bax/Bak and activation of JNK. *Toxicol. Appl. Pharmacol.* **203:** 124–131; 2005.
[16] Jiang, X.; Wang, X. Cytochrome c-mediated apoptosis. *Annu. Rev. Biochem.* **73:** 87–106; 2004.
[17] Vander Heiden, M. G.; Thompson, C. B. Bcl-2 proteins: regulators of apoptosis or of mitochondrial homeostasis? *Nat. Cell Biol.* **1:**E209–216; 1999.
[18] Kaufman, R. J. Stress signaling from the lumen of the endoplasmic reticulum: coordination of gene transcriptional and translational controls. *Genes Dev.* **13:** 1211–1233; 1999.
[19] Patil, C.; Walter, P. Intracellular signaling from the endoplasmic reticulum to the nucleus: the unfolded protein response in yeast and mammals. *Curr. Opin. Cell Biol.* **13:**349–355; 2001.
[20] Ferri, K. F.; Kroemer, G. Organelle-specific initiation of cell death pathways. *Nat. Cell Biol.* **3:**E255–263; 2001.
[21] Zinszner, H.; Kuroda, M.; Wang, X.; Batchvarova, N.; Lightfoot, R. T.; Remotti, H.; Stevens, J. L.; Ron, D. CHOP is implicated in programmed cell death in response to impaired function of the endoplasmic reticulum. *Genes Dev.* **12:**982–995; 1998.
[22] Oyadomari, S.; Mori, M. Roles of CHOP/GADD153 in endoplasmic reticulum stress. *Cell Death Differ.* **11:**381–389; 2004.

[23] Friedman, A. D. GADD153/CHOP, a DNA damage-inducible protein, reduced CAAT/enhancer binding protein activities and increased apoptosis in 32D c13 myeloid cells. *Cancer Res.* **56:**3250–3256; 1996.
[24] Lee, J. H.; Li, Y. C.; Ip, S. W.; Hsu, S. C.; Chang, N. W.; Tang, N. Y.; Yu, C. S.; Chou, S. T.; Lin, S. S.; Lino, C. C.; Yang, J. S.; Chung, J. G. The role of Ca^{2+} in baicalein-induced apoptosis in human breast MDA-MB-231 cancer cells through mitochondria- and caspase-3-dependent pathway. *Anticancer Res.* **28:**1701–1711; 2008.
[25] Yeh, T. C.; Chiang, P. C.; Li, T. K.; Hsu, J. L.; Lin, C. J.; Wang, S. W.; Peng, C. Y.; Guh, J. H. Genistein induces apoptosis in human hepatocellular carcinomas via interaction of endoplasmic reticulum stress and mitochondrial insult. *Biochem. Pharmacol.* **73:** 782–792; 2007.
[26] Suganuma, M.; Kurusu, M.; Suzuki, K.; Tasaki, E.; Fujiki, H. Green tea polyphenol stimulates cancer preventive effects of celecoxib in human lung cancer cells by upregulation of GADD153 gene. *Int. J. Cancer* **119:**33–40; 2006.
[27] Woo, K. J.; Lee, T. J.; Lee, S. H.; Lee, J. M.; Seo, J. H.; Jeong, Y. J.; Park, J. W.; Kwon, T. K. Elevated gadd153/chop expression during resveratrol-induced apoptosis in human colon cancer cells. *Biochem. Pharmacol.* **73:**68–76; 2007.
[28] McCullough, K. D.; Martindale, J. L.; Klotz, L. O.; Aw, T. Y.; Holbrook, N. J. Gadd153 sensitizes cells to endoplasmic reticulum stress by down-regulating Bcl2 and perturbing the cellular redox state. *Mol. Cell. Biol.* **21:**1249–1259; 2001.
[29] Puthalakath, H.; O'Reilly, L. A.; Gunn, P.; Lee, L.; Kelly, P. N.; Huntington, N. D.; Hughes, P. D.; Michalak, E. M.; McKimm-Breschkin, J.; Motoyama, N.; Gotoh, T.; Akira, S.; Bouillet, P.; Strasser, A. ER stress triggers apoptosis by activating BH3-only protein Bim. *Cell* **129:**1337–1349; 2007.
[30] Dharmaratne, H. R.; Nanayakkara, N. P.; Khan, I. A. Kavalactones from Piper methysticum, and their ^{13}C NMR spectroscopic analyses. *Phytochemistry* **59:** 429–433; 2002.
[31] Lin, C. J.; Wu, K. H.; Yew, F. H.; Lee, T. C. Differential cytotoxicity of cadmium to rat embryonic fibroblasts and human skin fibroblasts. *Toxicol. Appl. Pharmacol.* **133:** 20–26; 1995.
[32] Lin, Y. W.; Chuang, S. M.; Yang, J. L. Persistent activation of ERK1/2 by lead acetate increases nucleotide excision repair synthesis and confers anti-cytotoxicity and anti-mutagenicity. *Carcinogenesis* **24:**53–61; 2003.
[33] Jiang, H. Y.; Wek, R. C. Phosphorylation of the alpha-subunit of the eukaryotic initiation factor-2 (eIF2alpha) reduces protein synthesis and enhances apoptosis in response to proteasome inhibition. *J. Biol. Chem.* **280:**14189–14202; 2005.
[34] Wang, X. Z.; Ron, D. Stress-induced phosphorylation and activation of the transcription factor CHOP (GADD153) by p38 MAP kinase. *Science* **272:** 1347–1349; 1996.
[35] Maytin, E. V.; Ubeda, M.; Lin, J. C.; Habener, J. F. Stress-inducible transcription factor CHOP/gadd153 induces apoptosis in mammalian cells via p38 kinase-dependent and -independent mechanisms. *Exp. Cell Res.* **267:**193–204; 2001.
[36] SarKar, S.; Su, Z. Z.; Lebedeva, I. V.; Sauane, M.; Gopalkrishnan, R. V.; Valerie, K.; Dent, P.; Fisher, P. B. *mda*-7 (IL-24) mediates selective apoptosis in human melanoma cells by inducing the coordinated overexpression of the GADD family of genes by means of p38 MAPK. *Proc. Natl. Acad. Sci. U. S. A.* **99:**10054–10059; 2002.
[37] Oh-Hashi, K.; Maruvama, W.; Isobe, K. Peroxynitrite induces GADD34, 45, and 153 via p38 MAPK in human neuroblastoma. *Free Radic. Biol. Med.* **30:**213–221; 2001.
[38] Benali-Furet, N. L.; Chami, M.; Houel, L.; De Giorgi, F.; Vernejoul, F.; Lagorce, D.; Buscail, L.; Bartenschlager, R.; Ichas, F.; Rizzuto, R.; Paterlini-Bréchot, P. Hepatitis C virus core triggers apoptosis in liver cells by inducing ER stress and ER calcium depletion. *Oncogene* **24:**4921–4933; 2005.
[39] Liu, T.; Laurell, C.; Selivanova, G.; Lundeberg, J.; Nilsson, P.; Wiman, K. G. Hypoxia induces p53-dependent transactivation and Fas/CD95-dependent apoptosis. *Cell Death Differ.* **14:**411–421; 2007.
[40] Guan, L.; Han, B.; Li, Z.; Hua, F.; Huang, F.; Wei, W.; Yang, Y.; Xu, C. Sodium selenite induces apoptosis by ROS-mediated endoplasmic reticulum stress and mitochondrial dysfunction in human acute promyelocytic leukemia NB4 cells. *Apoptosis* **14:** 218–225; 2009.
[41] Yokouchi, M.; Hiramatsu, N.; Hayakawa, K.; Okamura, M.; Du, S.; Kasai, A.; Takano, Y.; Shitamura, A.; Shimada, T.; Yao, J.; Kitamura, M. Involvement of selective reactive oxygen species upstream of proapoptotic branches of unfolded protein response. *J. Biol. Chem.* **283:**4252–4260; 2008.
[42] Tagawa, Y.; Hiramatsu, N.; Kasai, A.; Hayakawa, K.; Okamura, M.; Yao, J.; Kitamura, M. Induction of apoptosis by cigarette smoke via ROS-dependent endoplasmic reticulum stress and CCAAT/enhancer-binding protein-homologous protein (CHOP). *Free Radic. Biol. Med.* **45:**50–59; 2008.
[43] Lim, S. T. S.; Dragull, K.; Tang, C. S.; Bittenbender, H. C.; Efird, J. T.; Nerurkar, P. V. Effects of kava alkloid, pipermethystine, and kavalactones on oxidative stress and cytochrome p450 in F-344 rats. *Toxicol. Sci.* **97:**214–221; 2007.
[44] Khan, N.; Afaq, F.; Syed, D. N.; Mukhtar, H. Fiestin, a novel dietary flavonoid, causes apoptosis and cell cycle arrest in human prostate cancer LNCaP cells. *Carcinogenesis* **29:**1049–1056; 2008.
[45] Tang, Y.; Simoneau, A. R.; Xie, J.; Shahandeh, B.; Zi, X. Effects of the kava chalcone flavokawain A differ in bladder cancer cells with wild-type versus mutant p53. *Cancer Prev. Res. (Philadelphia)* **1:**439–451; 2008.
[46] Yang, H. L.; Chen, S. C.; Chen, C. S.; Wang, S. Y.; Hseu, Y. C. Alpinia pricei rhizome extracts induce apoptosis of human carcinoma KB cells via a mitochondria-dependent apoptotic pathway. *Food Chem. Toxicol.* **46:**3318–3324; 2008.
[47] Yu, Y. S.; Hsu, C. L.; Yen, G. C. Anti-inflammatory effects of the roots of Alpinia Hayato and its phenolic compounds. *J. Agric. Food Chem.* **57:**7673–7680; 2009.
[48] Morré, D. J.; Chueh, P. J.; Morré, D. M. Capsaicin inhibits preferentially the NADH oxidase and growth of transformed cells in culture. *Proc. Natl. Acad. Sci. U. S. A.* **92:** 1831–1835; 1995.
[49] Wang, Y. C.; Bachrach, U. The specific anti-cancer activity of green tea (−)-epigallocatechin-3-gallate (EGCg). *Amino Acids* **22:**131–143; 2002.
[50] Ran, Z. H.; Xu, Q.; Tong, J. L.; Xiao, S. D. Apoptotic effect of epigallocatechin-3-gallate on the human gastric cancer cell line MKN45 via activation of the mitochondrial pathway. *World J. Gastroenterol.* **13:**4255–4259; 2007.
[51] Lu, H. F.; Hsueh, S. C.; Ho, Y. T.; Kao, M. C.; Yang, J. S.; Chiu, T. H.; Huang, S. Y.; Lin, C. C.; Chung, J. G. ROS mediates baicalin-induced apoptosis in human promyelocytic leukemia HL-60 cells through the expression of the Gadd153 and mitochondrial-dependent pathway. *Anticancer Res.* **27:**117–125; 2007.
[52] Newcomb, E. W.; Tamasdan, C.; Entzminger, Y.; Alonso, J.; Friedlander, D.; Crisan, D.; Miller, D. C.; Zagzag, D. Flavopiridol induces mitochondrial-mediated apoptosis in murine glioma GL261 cells via release of cytochrome c and apoptosis inducing factor. *Cell Cycle* **2:**243–250; 2003.
[53] Siegelin, M. D.; Reuss, D. E.; Habel, A.; Herold-Mende, C.; von Deimling, A. The flavonoid kaempferol sensitizes human glioma cells to TRAIL-mediated apoptosis by proteasomal degradation of survivin. *Mol. Cancer Ther.* **7:**3566–3574; 2008.
[54] Horinaka, M.; Yoshida, T.; Shiraishi, T.; Nakata, S.; Wakada, M.; Nakanishi, R.; Nishino, H.; Matsui, H.; Sakai, T. Luteolin induces apoptosis via death receptor 5 upregulation in human malignant tumor cells. *Oncogene* **24:**7180–7189; 2005.
[55] O'Connor, L.; Strasser, A.; O'Reilly, L. A.; Hausmann, G.; Adams, J. M.; Cory, S.; Huang, D. C. Bim: a novel member of the Bcl-2 family that promotes apoptosis. *EMBO J.* **17:**384–395; 1998.
[56] Copanaki, E.; Schümann, T.; Eckert, A.; Leuner, K.; Müller, W. E.; Prehn, J. H.; Köqel, D. The amyloid precursor protein potentiates CHOP induction and cell death in response to ER Ca^{2+} depletion. *Biochim. Biophys. Acta* **1773:**157–165; 2007.
[57] Shukla, S.; Gupta, S. Apigenin-induced prostate cancer cell death is initiated by reactive oxygen species and p53 activation. *Free Radic. Biol. Med.* **44:**1833–1845; 2008.
[58] Lu, H. F.; Hsueh, S. C.; Ho, Y. T.; Kao, M. C.; Yang, J. S.; Chiu, T. H.; Huamg, S. Y.; Lin, C. C.; Chung, J. G. ROS mediates baicalin-induced apoptosis in human promyelocytic leukemia HL-60 cells through the expression of the GADD153 and mitochondrial-dependent pathway. *Anticancer Res.* **27:**117–125; 2007.
[59] Psahoulia, F. H.; Moumtzi, S.; Roberts, M. L.; Sasazuki, T.; Shirasawa, S.; Pintzas, A. Quercetin mediates preferential degradation of oncogenic Ras and causes autophagy in Ha-RAS-transformed human colon cells. *Carcinogenesis* **28:** 1021–1031; 2007.
[60] Longo, L.; Platini, F.; Scardino, A.; Alabiso, O.; Vasapollo, G.; Tessitore, L. Autophagy inhibition enhances anthocyanin-induced apoptosis in hepatocellular carcinoma. *Mol. Cancer Ther.* **7:**2476–2485; 2008.
[61] Tang, Y.; Li, X.; Liu, Z.; Simoneau, A. R.; Xie, J.; Zi, X. Flavokawain B, a kava chalcone, induces apoptosis via up-regulation of death-receptor 5 and Bim expression in androgen receptor negative, hormonal refractory prostate cancer cell lines and reduces tumor growth. Int. J. Cancer. doi:10.1002/ijc.25210.
[62] Li, N.; Liu, J. H.; Zhang, J.; Yu, B. Y. Comparative evaluation of cytotoxicity and antioxidative activity of 20 flavonoids. *J. Agric. Food Chem.* **56:**3876–3883; 2008.
[63] Lin, C. T.; Senthil Kumar, K. J.; Tseng, Y. H.; Wang, Z. J.; Pan, M. Y.; Xiao, J. H.; Chien, S. C.; Wang, S. Y. Anti-inflammatory activity of flavokawain B from Alpinia pricei Hayato. *J. Agric. Food Chem.* **57:**6060–6065; 2009.